

## C-band Frequency Generator for Space-Borne Synthetic Aperture Radar

Nidhi Singh\*, Jolly Dhar, Cheemalamarri V. N. Rao, and Gurleen S. Rajpal

**Abstract**—This paper presents the design and implementation of a C-Band Frequency Generator developed for Space-borne Synthetic Aperture Radar. This Frequency Generator subsystem generates stable and coherent reference signals for all the sub-systems of C-Band Synthetic Aperture Radar payload. Frequency Generator based on frequency multiplication technique generates various coherent signals namely 500 MHz signal for digital clock, local oscillator (LO) signals of 900 MHz and 4500 MHz needed for receivers and chirp signal of  $5400 \pm 37.5$  MHz. This chirp signal is generated by direct modulation of the full bandwidth baseband signal of DC-37.5 MHz at 4500 MHz and subsequently mixing with 900 MHz signal. Frequency generator unit is realized in a compact two-tier architecture, using a novel concept of full chirp modulation, resulting in  $6^\circ$  rms phase error in the transmit chirp signal along with in-band spurious rejection better than 20 dBc, whereas other coherent frequencies resulting in out of band spurious rejection better than 53 dBc against the specification of 40 dBc.

### 1. INTRODUCTION

Synthetic Aperture Radar (SAR) is an extremely important microwave sensor having the advantage of height-independent resolution capability along with all-weather, day and night imaging capabilities [1]. It caters to diverse applications like agriculture, forestry, geology, hydrology, disaster-monitoring, cryosphere, oceanography, and archaeological applications. As per prior art [2] by Misra et al. and [3] by Rao et al., C-Band Linear Frequency Modulation (LFM) signal generation using multiplication scheme is reported. This is qualified for space applications. In [4], a fast-switching carrier frequency generator for multi-band ultra-wideband (UWB) radios is presented by Mishra et al. It is based on the generation of multi-spot frequencies, but no chirp generation is involved in this reported work. In [5], Huang et al. present Frequency Modulated Continuous Wave (FMCW) radar transmitter at 4.1 to 4.5 GHz suitable for long-distance detection using 180-nm CMOS process. Madiwalesh et al. have discussed C-band frequency synthesizer developed to test the performance of a RADAR in [6]. C-band SAR is an active phased array antenna based multimode SAR payload, and its hardware is functionally divided into transmitter, receiver, active antenna, and digital subsystems. In transmitter, digitally generated baseband chirp signal is up-converted to C-band in Frequency Generator (FG) and further amplified to desired level. FG is a coherent subsystem which not only generates the modulated chirp transmit signal but also does the time synchronization of the payload by providing clock signals and Local Oscillator (LO) signals required for demodulation in receiver. In FG, as a coherent source 50 MHz Temperature Compensated Crystal Oscillator (TCXO) is used, due to which discrete spurious signals are present in the spectrum which are 50 MHz away from the desired carrier frequency viz. 500 MHz, 900 MHz, and 4500 MHz signals. The unwanted spurious signals are rejected by using sharp cut-off band-pass filters at the output of TCXO and output of various multipliers. Thermal and structural analysis is done to meet the temperature and package integrity.

---

*Received 30 June 2023, Accepted 6 September 2023, Scheduled 22 September 2023*

\* Corresponding author: Nidhi Singh (nidhi@sac.isro.gov.in).

The authors are with the Space Applications Centre, ISRO, DOS, Ahmedabad, India.

## 2. NOVEL DESIGN APPROACH

The frequency generator presented here is a complex subsystem containing a huge number of active gain modules, distributed over a gamut of frequencies ranging from 50 MHz to 5.4 GHz. The outputs of FG include clock signal, LO frequency, a full bandwidth (75 MHz) chirp generation without any post-modulation multiplication. The absence of post modulation multiplication stage has resulted in reduced phase error of the subsystem. The more the reduction is in phase error, the better the transmitting chirp quality is as transmitting chirp phase approaches to ideal quadratic condition. Better amplitude flatness and reduced phase error resulted in minimised side lobes of final payload response, thus improving peak side lobe ratio (PSLR) and integrated side lobe ratio (ISLR). The spurious rejection requirements have been met by the use of filtering in multiple stages. The cavity sizes in package have been carefully selected so as to avoid unwanted coupling at the frequency range of interest. The analytical expression for the resonant frequencies based on the theoretical analysis is given in Eq. (1).

$$f_{mnp} = \frac{c}{2\pi\sqrt{\mu_r\epsilon_r}} \sqrt{\left(\frac{m\pi}{a}\right)^2 + \left(\frac{n\pi}{b}\right)^2 + \left(\frac{p\pi}{d}\right)^2} \quad (1)$$

Here,  $\mu_r$  is the complex relative permeability,  $\epsilon_r$  the complex relative permittivity,  $a$  the width,  $b$  the height,  $d$  the length, and  $m$ ,  $n$ , and  $p$  are mode numbers. Cavity analysis is done for multiple cavities and shown in Table 1. Cavities of FG have been designed using Equation (1) as well as cavity analysis done by High Frequency Structural Simulator [7].

**Table 1.** Analysis of multiple cavities of FG.

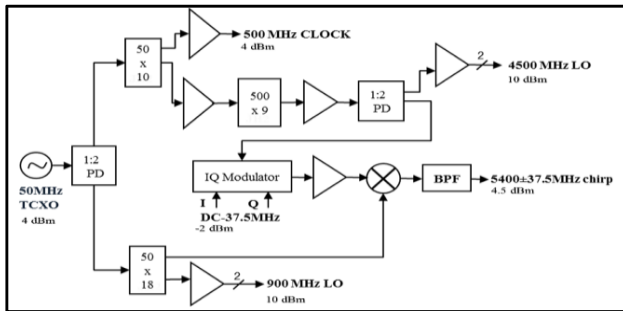
Cavity	Fundamental Resonance Frequency (GHz)		Highest operating frequency
	Theoretical	Analysis	
Amplifier Cavity	7.0	7.1	5.5 GHz
Multiplier Cavity	5.1	5.2	4.5 GHz
Filter Cavity	7.0	7.1	5.5 GHz
Power Divider Cavity	5.2	5.3	4.5 GHz
IQ Modulator Cavity	5.5	5.6	4.5 GHz

Table 1 depicts that maximum operating frequency is below the worst-case fundamental resonance frequency, hence practically no cavity resonance. Further, double cover approach has been adopted to avoid the coupling of undesired signal. In all designs, mitering of RF path bends is done for the smooth flow of RF signal. Electromagnetic Interference (EMI) Gasket on outer covers, depressed cavity for all SMA RF connectors, RF bypass capacitors in DC path, high-Q RF coupling capacitors in RF path, DC harness with twisted pairs, and EMI line filters in supplies are used to avoid any electromagnetic interference [8, 9].

## 3. DESIGN METHODOLOGY

The reported FG subsystem generates multiple coherent frequency signals from a stable 50 MHz TCXO used as a reference source. The 50 MHz reference signal is used to generate Clock Output at 500 MHz, 900 MHz LO, 4500 MHz LO, and  $(5400 \pm 37.5)$  MHz modulated chirp signal using frequency multiplication and mixing technique. The block schematic of Frequency Generator is shown in Fig. 1. The two-way power dividers used in FG are designed using Wilkinson topology, which is widely used in many microwave systems to get desired isolation [10]. In proposed FG, 20 dB minimum isolation is maintained between output ports of power divider. Small signal amplifiers are designed using Bipolar Junction Transistor (BJT) and Field Effective Transistor (FET) devices for maximum gain design because of unconditional stability. In order to meet the specifications of spurious and harmonic rejection at the outputs, band-pass filters and low-pass filters have been used at appropriate places. Band-pass

filters are designed based on split ring resonator and parallel coupled line topology. Multipliers can be designed using active devices FETs [11–13] or BJTs. In this reported paper, BJTs are used for multipliers viz. 50 MHz X10, 50 MHz X17, 500 MHz X9. BJTs are used due to their higher stability and ease of input and output matching at lower frequencies as compared to FETs. Further to improve the noise performance, a low noise BJT device is used for noise suppression better than 75 dBc around carrier frequency. This gives noise reduction at higher output frequency than extracting harmonics from narrow pulse [14]. This noise suppression is very much important to incorporate at the end of FG; otherwise, the noise will mask demodulated response up to a few MHz bandwidth. Device operating point is chosen such that optimum conduction angle can be achieved, and the desired harmonic at output is obtained. Apart from the desired output frequency, all other harmonics are suppressed using band-pass filter at the output of multiplier. These circuits are fabricated on a 25 mil alumina substrate on a gold plated carrier plate made of Kovar material. In-Quadrature (IQ) phase modulator generates modulated signal at  $(4500 \pm 37.5)$  MHz when I and Q signal from DC-37.5 MHz baseband signal coming from digital domain is mixed with 4500 MHz LO signal. Subsequently,  $4500 \pm 37.5$  MHz signal is further mixed with 900 MHz signal to get desired  $(5400 \pm 37.5)$  MHz modulated chirp signal. IQ Modulator has intermediate frequency (IF) close to DC and high Local oscillator (LO) signal of 4.5 GHz [15]. IQ Modulator is designed using two single balanced mixers designed using beam lead Schottky diodes, rat race coupler, 90 deg hybrid [16], and power combiner. It gives good LO to RF isolation of 25 dB. It is fabricated on an RT6010 25 mil duroid substrate, attached on a gold plated carrier plate made of aluminium. In FG, the distribution of gain is suitably done to avoid oscillations in any cavity. EMI filters in each RF circuit are used to avoid any low frequency signal, which can cause oscillation. The complete FG package has been realized in a two-tier configuration integrated with its Electronic Power Conditioner (EPC) unit placed at the top of the package. The two RF trays of the FG package have Microwave Integrated Circuit (MIC) and Printed Circuit Board (PCB) on both sides. Semi-rigid cables are used for connecting both packages to minimize RF losses. Line filters are used in FG for filtering any low frequency signal to desired level. The integrated FG is shown in Fig. 2.



**Figure 1.** Block schematic of FG.

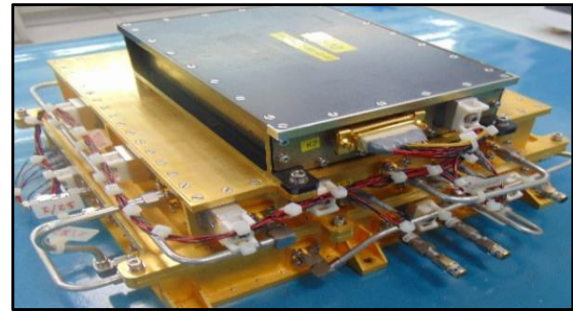


**Figure 2.** Integrated frequency generator.

Frequency Generator has been analysed for thermal as well as structural parameters. Thermal analysis is required to ascertain proper heat dissipation from FG. All the components viz. resistor, inductor, capacitor, active devices, feedthroughs are derated as per space guidelines to ensure efficient thermal management. Most importantly, active devices play an important role in thermal management. Their junction temperature [17] is calculated from following equation as,

$$T_j = T_a + \theta \cdot P_d \quad (2)$$

where  $T_j$  is the junction temperature,  $T_a$  an external temperature,  $\theta$  the thermal resistance, and  $P_d$  the dissipated power. For thermal analysis, material considered is Kovar for carrier plates of RF circuits, Aluminium Alloy Al6061 for Trays, FR-4 material for PCB cards to provide the dc voltages required for all the active devices. Bottom tray is mounted on a base plate with thermal grease to provide good thermal contact for efficient heat transfer. In the case of FG,  $T_a = 55^\circ\text{C}$  (worst case),  $\theta$  is 375 K/W,  $P_d = 72$  mW giving  $T_j = 82^\circ\text{C}$ . This is well below the specification of maximum junction temperature of  $110^\circ\text{C}$ . In this FG, very efficient power dissipation is distributed in package. So, it removes the need

of putting heat sink and hence reduced size and weight. Dissipation of complete FG package is 9 W. FG package is mechanically designed with H type configuration. Each tray consists of top and bottom covers, cavity covers, carrier plates, PCBs, interconnecting cables, and RF connectors. It has mass of 4.5 kg and size of  $\sim 235 \times 212 \times 112 \text{ mm}^3$ . Structural analysis of Frequency Generator is done to analyse steady state stress and random response in all axes and natural frequency. Modal analysis technique was performed to obtain the first natural frequency of FG which is 191.4 Hz. This is very well above specification of 100 Hz.

#### 4. MEASURED RESULTS

The unit has been tested in the temperature range from  $-15^\circ\text{C}$  to  $55^\circ\text{C}$ . Passive temperature compensation has been used to compensate for output power level variation with temperature. Time domain measurement is captured to characterise transmitting modulated LFM chirp for parameters namely chirp flatness, out of band sideband suppression ( $\sim 24 \text{ dBc}$ ) as depicted in Fig. 3. In Fig. 4, single tone spectrum of transmitting chirp signal is shown which is generated when 10 MHz lower side baseband signal is modulated with 4500 MHz LO and then mixed with mixer to get final signal. This final desired signal is at 5390 MHz along with 5400 MHz as leakage signal and other in-band spurious signals. Here, worst case in-band sideband suppression is 20 dBc which is acceptable for payload system performance. Direct modulation of the available full bandwidth baseband signal (DC-37.5 MHz) resulted in reduced phase error of  $6^\circ$  rms, improving transmitter LFM chirp quality.

Phase noise of all the signals has been measured, and short-term stability is derived, which is  $1.0 \times 10^{-10}$  at 1 s against specification of  $1.0 \times 10^{-9}$  at 1 s. Fig. 5 shows short term stability at 4500 MHz output signal. Long term stability of Frequency Generator is the same as the long term stability of TCXO used which in this case is  $\pm 0.5 \text{ ppm/year}$ . The spurious suppression in all continuous wave signals viz. 500 MHz clock signal, 900 MHz and 4500 MHz LO signals is better than the specification of 40 dBc as shown in Figs. 6, 7, and 8, respectively. Phase noise of 4500 MHz is shown in Fig. 9, Phase noise of 5400 MHz signal and 5390 MHz signal is shown in Fig. 10. Accordingly, specifications and comparison of Frequency Generator with respect to prior works are shown in Table 2.

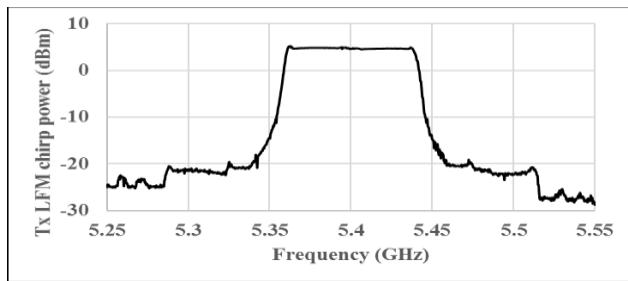


Figure 3. Profile of Tx LFM chirp.

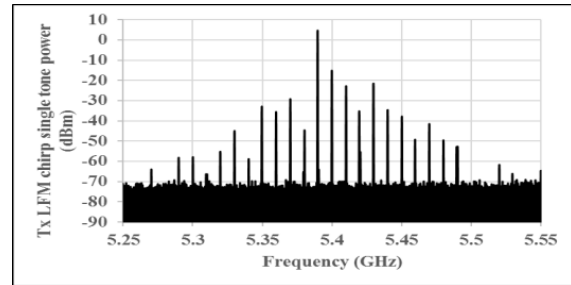


Figure 4. Single tone spectrum.

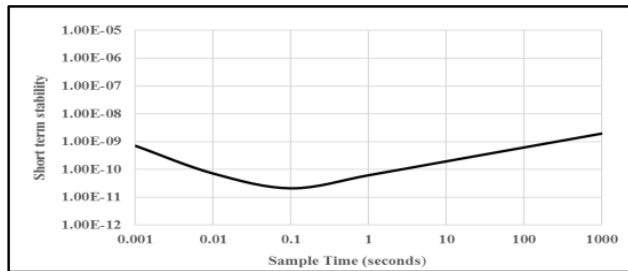


Figure 5. Short term stability @4500 MHz.

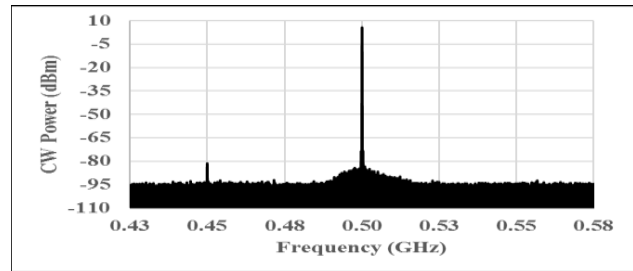


Figure 6. Spectrum of 500 MHz clock.

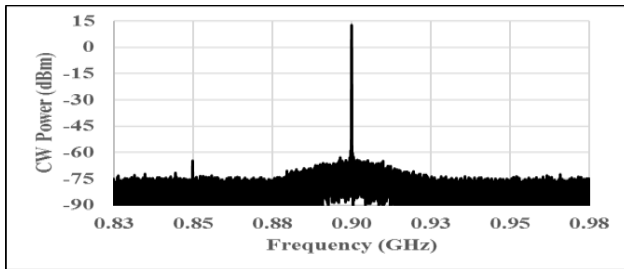


Figure 7. Spectrum of 900 MHz LO signal.

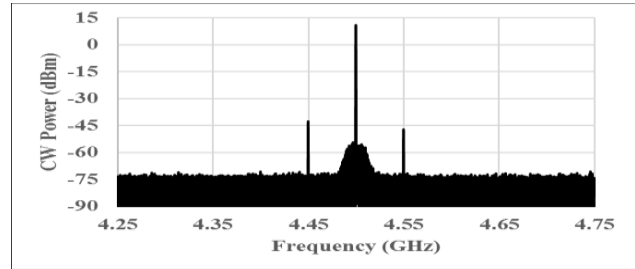


Figure 8. Spectrum of 4500 MHz LO signal.

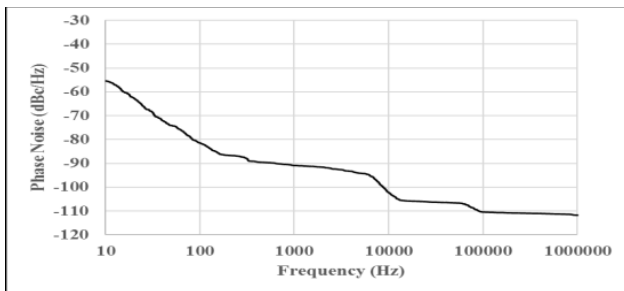


Figure 9. Phase noise of 4500 MHz.

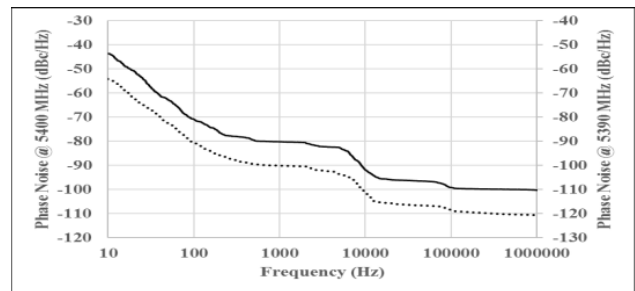


Figure 10. Phase noise of 5400 & 5390 MHz.

Table 2. Specifications and comparison of frequency generator.

Parameter	Specifications	[2] & [3]	[4]	[5]	[6]	This work
Clock signal Power	4 dBm min. @500 MHz	2 dBm @250 MHz	3.7–10 GHz, –26.5 dBm @4.752 GHz	4.1–4.5 GHz	C-Band, 4.43 dBm	5.5 dBm @500 MHz
LOs to Rx Power	10 dBm min. @900 & 4500 MHz	10 dBm @850 MHz, 8 dBm @4500 MHz				12 dBm @900 MHz, 11 dBm @4500 MHz
Transmit (Tx) Chirp power	0.5 dBm min. @5400 ± 37.5 MHz	0 dBm @5350 ± 125 MHz				4.5 dBm @5400 ± 37.5 MHz
Tx Chirp generation	—	Multiplication	—	—	—	Direct modulation
Tx Chirp Flatness	1 dB max. (75 MHz BW)	2 dB (225 MHz BW)	—	—	—	0.45 dB (75 MHz BW)
Tx Chirp Out of band Spurious suppression	20 dBc min.	20 dBc	—	—	—	24 dBc
Tx Chirp In-band Spurious suppression	20 dBc min.	20 dBc	18 dBc	—	—	20 dBc
Tx Chirp Phase error	—	13° rms	—	—	—	6° rms
Out of Band Spurious	> 40 dBc	> 50 dBc	> 30 dBc	—	73.85 dBc	> 53 dBc
Phase noise 10 kHz offset @4500 MHz	—	–107 dBc/Hz	—	–50 dBc/Hz	–123 dBc/Hz	–102 dBc/Hz
Phase noise 1 MHz offset @4500 MHz	—	—	—	–123 dBc/Hz	–130 dBc/Hz	–111 dBc/Hz
Short term stability	1.0e-9 @1 s	1.0e-10 @1 s	—	—	—	1.0e-10 @1 s
Space Qualification	—	Yes	No	No	No	Yes

## 5. CONCLUSION

The Frequency Generator designed and developed for C Band SAR, generates stable and coherent reference signals for all the sub-systems of C-Band SAR payload. Phase noise of all the signals has been measured, and the derived short-term stability is  $1.0\text{e-}10$  at 1 s against specification of  $1.0\text{e-}9$  at 1 s. The fabricated FG validates the requirement of spurious rejection in continuous wave signals and provides reduced phase error of  $6^\circ$  rms in Transmitter LFM chirp.

## REFERENCES

1. Moreira, A. and G. Krieger, "Spaceborne synthetic aperture radar (SAR) systems: State of art and future developments," *33rd European Microwave Conference Proceedings (IEEE Cat. No.03EX723C)*, IEEE, Munich, Germany, 2003.
2. Misra, T., S. S. Rana, N.M. Desai, et al., "Synthetic aperture radar payload on-board RISAT-1: Configuration, technology and performance," *Current Science Journal*, 2013.
3. Rao, Ch. V. N., B. V. Bakori, J. Dhar, et al., "RF and microwave subsystems for RISAT-1 SAR payload," *Signatures, Newsletter of the ISRS-AC*, Vol. 24, No. 2, Apr. 2012.
4. Mishra, C., A. V. Garcia, E. S. Sinencio, et al., "A carrier frequency generator for multi-band UWB radios," *IEEE Radio Frequency Integrated Circuits (RFIC) Symposium, 2006*, IEEE, San Francisco, CA, USA, 2006.
5. Huang, X., W. Deng, H. Jia, et al., "A C-band FMCW radar transmitter with a 22 dBm output power series-stacking CMCD PA for long-distance detection in 180-nm CMOS technology," *IEEE International Conference on Integrated Circuits, Technologies and Applications (ICTA)*, IEEE, Zhuhai, China, 2021.
6. Madiwalesh, M. P., M. S. Ruchit, M. V. Harikrishna, et al., "Design and development of agile C-band synthesizer for RADAR," *2018 IEEE MTT-S International Microwave and RF Conference (IMaRC)*, IEEE, Kolkata, India, 2018.
7. Ansoft High frequency Structure Simulator, Version 17, User's manual.
8. Dhar, J., "Enclosure effect on microwave power amplifier," *Progress In Electromagnetics Research C*, Vol. 19, 163–177, 2011.
9. Dhar, J., S. K. Garg, R. K. Arora, B. V. Bakori, and S. S. Rana, "C-band pulsed solid state power amplifier for spaceborne applications," *Progress In Electromagnetics Research Letters*, Vol. 23, 75–87, 2011.
10. Bin Muhammad Nor, M. Z., S. K. Abdul Rahim, M. I. bin Sabran, and M. S. bin Abdul Rani, "Wideband planar Wilkinson power divider using double-sided parallel-strip line technique," *Progress In Electromagnetics Research C*, Vol. 36, 181–193, 2013.
11. Srivastava, S., G. V. Reddy, J. Dhar, et al., "Active frequency doubler at X-band," *2022 IEEE Microwaves, Antennas, and Propagation Conference (MAPCON)*, IEEE, Bangalore, India, 2022.
12. Camargo, E., *Design of FET Frequency Multipliers and Harmonic Oscillators*, Artech House, 1998.
13. Klymyshyn, D. M. and Z. Ma, "Active frequency-multiplier design using CAD," *IEEE Transactions on Microwave Theory and Techniques*, Vol. 51, No. 4, Apr. 2003.
14. Zhou, M., S. Tang, W. Wang, et al., "A frequency multiplication method based on extracting harmonic from narrowpulse," *IEEE Access*, Jul. 2019.
15. Mishra, S., N. Singh, J. Dhar, et al., "A GaAs based miniaturized C-band double balanced resistive IQ modulator for synthetic aperture radar (SAR) applications," *IEEE Recent Advances in Geoscience and Remote Sensing: Technologies, Standards and Applications (TENGARSS)*, 2019.
16. Agrawal, G., P. Sinha, J. Dhar, et al., "Design and development of broadband and compact size IQ demodulator at  $850 \pm 112.5$  MHz," *6th International Conference for Convergence in Technology (I2CT)*, Apr. 2–4, 2021.
17. Scott, A. W., *Cooling of Electronic Equipment*, John Wiley & Sons, 1974.